

# Stochastic Dynamics of Growing Young Diagrams and Their Limit Shapes

P. L. Krapivsky<sup>1</sup>

<sup>1</sup>*Department of Physics, Boston University, Boston, MA 02215, USA*

We investigate a class of growing two-dimensional Young diagrams parametrized by a non-negative integer  $r$ , the minimal difference between the heights of adjacent columns. The limit shapes emerging in the long time limit are analytically determined, and fluctuations of the height and the width are briefly discussed. We also analyze the generalization to ‘diffusively’ growing Young diagrams.

## I. INTRODUCTION

Partitions of integers appear in various branches of mathematics, especially in combinatorics, number theory and group representations [1–8], and also in physics [9–16]. By definition, a partition of a natural number  $n$  is its representation as a sum

$$n = m_1 + \dots + m_k, \quad m_1 \geq \dots \geq m_k > 0 \quad (1)$$

The total number of partitions of  $n$  is denoted by  $p(n)$ . For instance,  $4 = 4$ ,  $4 = 3 + 1$ ,  $4 = 2 + 2$ ,  $4 = 2 + 1 + 1$  and  $4 = 1 + 1 + 1 + 1$  are all possible partitions of 4. Therefore  $p(4) = 5$ .

The study of partitions goes back to Euler [1]. One his famous result is the beautiful expression of the generating function encoding the sequence  $p(n)$  through a neat infinite product

$$\sum_{n \geq 0} p(n) q^n = \prod_{k \geq 1} \frac{1}{1 - q^k} \quad (2)$$

(It is convenient to set  $p(0) = 1$ .) Using (2) one can deduce the large  $n$  asymptotic  $\ln p(n) \simeq 2\pi\sqrt{n/6}$ . A more precise asymptotic formula by Hardy and Ramanujan [2]

$$p(n) \simeq \frac{1}{4\sqrt{3}n} \exp\left[\pi\sqrt{\frac{2n}{3}}\right]$$

and an exact Hardy-Ramanujan-Rademacher formula [3] have been derived (see e.g. [4]) via a connection of the generating function (2) with Dedekind’s eta function.

One can think about partitions geometrically representing them by Young diagrams (Fig. 1); e.g. the Young diagram of the partition (1) has  $k$  columns, with  $m_j$  being the height of the  $j^{\text{th}}$  column. The total number  $\mathbb{Y}_2(n)$  of Young diagrams composed of  $n$  elemental squares is  $\mathbb{Y}_2(n) = p(n)$ . Rather than fixing area, one can impose other restrictions, e.g. one can consider Young diagrams that fit into an  $a \times b$  box. The total number of such diagrams is  $\mathbb{Y}(a, b) = (a + b)! / [a! b!]$ .

The Young diagram is a two-dimensional (lattice) object, and it admits an obvious generalization to higher dimensions. The analog of Eq. (2) is known in three (but not higher) dimensions [5, 7, 17]:

$$\sum_{n \geq 0} \mathbb{Y}_3(n) q^n = \prod_{k \geq 1} \frac{1}{(1 - q^k)^k} \quad (3)$$

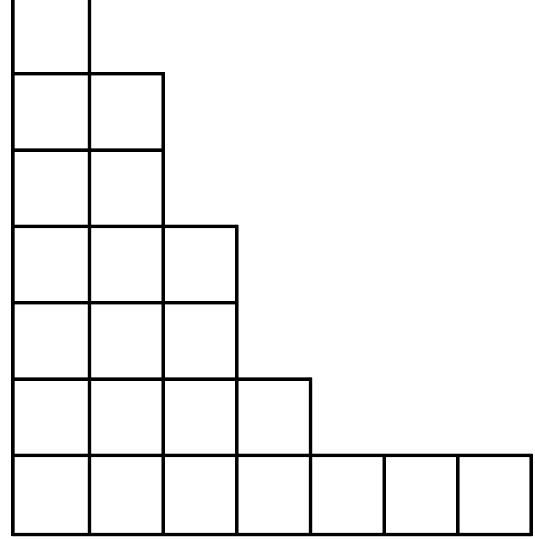


FIG. 1: A Young diagram of a partition of a positive integer  $n$  is a diagram with  $n$  boxes arranged in columns with non-increasing height. Shown is the Young diagram of the partition  $22 = 7 + 6 + 4 + 2 + 1 + 1 + 1$ .

where  $\mathbb{Y}_3(n)$  is the total number of three-dimensional Young diagrams of ‘volume’  $n$ . This expression via an infinite product was discovered by MacMahon [17] who also found a beautiful formula for the total number  $\mathbb{Y}(a, b, c)$  of Young diagrams that fit into an  $a \times b \times c$  box [7, 17]

$$\mathbb{Y}(a, b, c) = \prod_{i=1}^a \prod_{j=1}^b \prod_{k=1}^c \frac{i + j + k - 1}{i + j + k - 2} \quad (4)$$

The total number  $p(n)$  of partitions rapidly grows with  $n$ , yet for large  $n$  partitions are mostly similar, namely their Young diagrams look alike. To make this assertion precise one must define the probability measure. The simplest choice is the *uniform* probability measure postulating that all  $p(n)$  partitions of  $n$  are equiprobable. The limit shape emerges after rescaling the coordinates

$$X = \frac{j}{\sqrt{n}}, \quad Y = \frac{m_j}{\sqrt{n}} \quad (5)$$

and taking the  $n \rightarrow \infty$  limit while keeping  $X$  and  $Y$





The limit shape (6) is symmetric with respect to the reflection  $X \leftrightarrow Y$ , and its span is infinite along both axes. [From (6) one finds that the span grows logarithmically,  $X_* = Y_* = \frac{\sqrt{6}}{2\pi} \ln(n)$ , so it diverges in the  $n \rightarrow \infty$  limit.] The reflection symmetry is broken for the limit shape (21) and the horizontal span of the partition is finite:

$$X \leq X_* = \frac{\sqrt{12} \ln 2}{\pi} \quad (22)$$

In the original coordinates

$$j \leq j_* = \frac{\ln 2}{\pi} \sqrt{12n}$$

for  $n \gg 1$ . The maximal horizontal span is  $j_{\max} \approx \sqrt{2n}$ , it arises for the least tilted partition with strictly decreasing heights:  $j_{\max}, j_{\max} - 1, \dots, 1$ . Almost all strict partitions, however, are substantially more narrow:

$$\frac{j_*}{j_{\max}} = \frac{\sqrt{6} \ln 2}{\pi} = 0.54044463946673 \dots$$

We now turn to growing strict partitions which is our main subject. The first deposition event is the same as before, viz. (8) in the lattice gas framework. The second deposition events is also unique for strict partitions:

$$\bullet \bullet \bullet \bullet \bullet \circ \circ \circ \circ \circ \Rightarrow \bullet \bullet \bullet \bullet \bullet \circ \circ \circ \circ \quad (23)$$

The third deposition event is described by (10), both outcomes occur with the same probability. Analyzing (23), (10) and following deposition events one finds that the underlying lattice gas is a facilitated totally asymmetric simple exclusion process (FTASEP). This is an exclusion process (at most one particle per site), the adjective ‘simple’ refers to the fact that only nearest neighbor hopping is allowed, and only to the right (hence asymmetric). The crucial difference from the TASEP is facilitation, a particle can hop only when it is pushed from the left (that is, its neighboring left site is occupied).

For the FTASEP we also use the continuity equation (12) on the hydrodynamic level. The FTASEP and closely related models were studied in the past (see e.g. [42–48]) and the current is known:

$$J(n) = \frac{(1-n)(2n-1)}{n} \quad (24)$$

The solution (12)–(13) subject to the initial condition (14) is also known [48]:

$$N(Z) = \begin{cases} 1 & Z < -1 \\ (2+Z)^{-1/2} & -1 < Z < 1/4 \\ 0 & Z > 1/4 \end{cases} \quad (25)$$

In contrast to shock waves, rarefaction waves usually exhibit a continuous (although not smooth) dependence on coordinate. The rarefaction wave (25) is exceptional, the density jumps from  $N = \frac{2}{3}$  at  $Z = \frac{1}{4} - 0$  to  $N = 0$  at  $Z = \frac{1}{4} + 0$  (see Fig. 2).

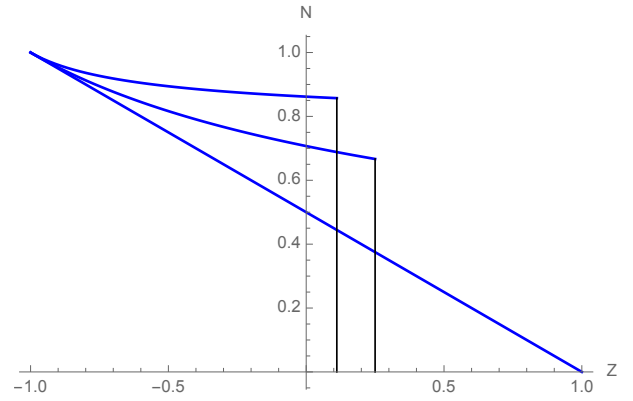


FIG. 2: The bottom curve is the rarefaction wave (15), the middle curve is the rarefaction wave (25) and the top curve is the rarefaction wave given by Eq. (33) with  $r = 4$ . The rarefaction waves (33) with  $r > 0$  have a discontinuity on the right edge  $Z = V(r)$ ; in the presented examples  $V(1) = \frac{1}{4}$  and  $V(4) = \frac{1}{9}$ .

The limit shape is found by using (16) which in the present case becomes

$$Y = \int_{\max(X-Y, -1)}^{1/4} dZ N(Z) \quad (26)$$

in the re-scaled coordinates (17). Combining (25) and (26) we determine the limit shape (see also Fig. 3)

$$Y = 1 - 2\sqrt{X} \quad (27)$$

Equation (27) gives the non-trivial parabolic part of the limit shape in the region  $0 < X < \frac{1}{4}$ ,  $0 < Y < 1$ .

#### IV. GENERAL CASE

In this section we look at  $r$ -strict partitions, viz. partitions satisfying the requirement  $m_j - m_{j+1} \geq r$ , where  $r$  is a fixed non-negative integer. (The last height is unrestricted:  $m_k \geq 1$ .) Unrestricted partitions are recovered when  $r = 0$ , while strict partitions correspond to  $r = 1$ .

The equilibrium case was studied in Refs. [49, 50]. The generalization of (6) and (21) reads

$$e^{\lambda r X} - e^{-\lambda Y} = e^{\lambda(r-1)X} \quad (28)$$

The parameter  $\lambda = \lambda(r)$  is found [49, 50] by requiring that the area under the curve (28) is equal to one:

$$\lambda^2 = \frac{\pi^2}{6} - \text{Li}_2(\rho) - \frac{r}{2} (\ln \rho)^2 \quad (29)$$

where  $\rho = \rho(r)$  is determined from  $\rho + \rho^r = 1$ . Here  $\text{Li}_2(\rho) = \sum_{k \geq 1} k^{-2} \rho^k$  is the dilogarithm function. For  $r = 0$  and  $r = 1$  one recovers the values given in (6) and (21), the next value is  $\lambda(2) = \pi/\sqrt{15}$ , etc.



which is asymptotically Gaussian with fluctuation on the scale  $t^{1/2}$ . Similarly the height is the displacement of the left-most vacancy, so it has the same Poisson distribution.

We now return to growing strict partitions and discuss fluctuations of the height and of the width. The former behaves as in the corner growth process:

$$\text{Prob}(h_t = n) = \frac{t^n}{n!} e^{-t} \quad (40)$$

The behavior of the width is harder to quantify since the right-most particle in the FTASEP hops only when it is pushed by its neighbor. Let us map the FTASEP onto a lattice gas [57, 58] in which a site corresponds to adjacent particles in the FTASEP, and it is empty ( $\square$ ) if adjacent particles are nearest neighbors and occupied ( $\blacksquare$ ) if there is a vacancy between adjacent particles. This is a one-to-one mapping since starting with initial condition (7) adjacent particles in the FTASEP will be separated by at most one vacancy. Note also that (7) corresponds to the empty half-line in the new lattice gas, see (41). Here is an example of the evolution (time goes from top to bottom)

$$\begin{array}{ll} \dots \bullet \bullet \bullet \bullet \bullet \circ \circ \circ \dots & \dots \square \square \square \square \\ \dots \bullet \bullet \bullet \bullet \bullet \circ \circ \circ \dots & \dots \square \square \square \blacksquare \\ \dots \bullet \bullet \bullet \circ \bullet \bullet \circ \circ \dots & \dots \square \square \square \blacksquare \\ \dots \bullet \bullet \bullet \circ \bullet \circ \bullet \circ \dots & \dots \square \square \blacksquare \blacksquare \\ \dots \bullet \bullet \bullet \circ \bullet \circ \bullet \circ \dots & \dots \square \blacksquare \blacksquare \blacksquare \\ \dots \bullet \bullet \circ \bullet \bullet \circ \bullet \circ \dots & \dots \square \blacksquare \square \blacksquare \\ \dots \bullet \bullet \circ \bullet \bullet \circ \bullet \circ \dots & \dots \square \blacksquare \blacksquare \square \end{array} \quad (41)$$

The lattice model shown on the right is the half-TASEP with particles hopping to the left and new particles entering the right-most site (both processes occur with unit rate). A simple but crucial observation immediately following from the above example is that the displacement  $w_t$  of the right-most particle for the FTASEP is the same as the total number of particles (denoted by  $\blacksquare$ ) in the half-TASEP.

For the TASEP starting with the initial condition (7) the total number of particles entering initially empty half line is given by (38). For the half-TASEP one expects that the total number of particles  $w_t$  entering initially empty half-line behaves similarly to (38). Fluctuations scale indeed as  $t^{1/3}$ , but they follow [58] the GSE Tracy-Widom distribution related to the Gaussian symplectic ensemble of random matrices:

$$w_t = \frac{t}{4} + t^{1/3} \mathcal{F}_{GSE} \quad (42)$$

The same  $\mathcal{F}_{GSE}$  appears in other growth processes in half-line [59–61], while the  $\mathcal{F}_{GUE}$  distribution describes fluctuations of the leading particle in a process studied in Ref. [62].

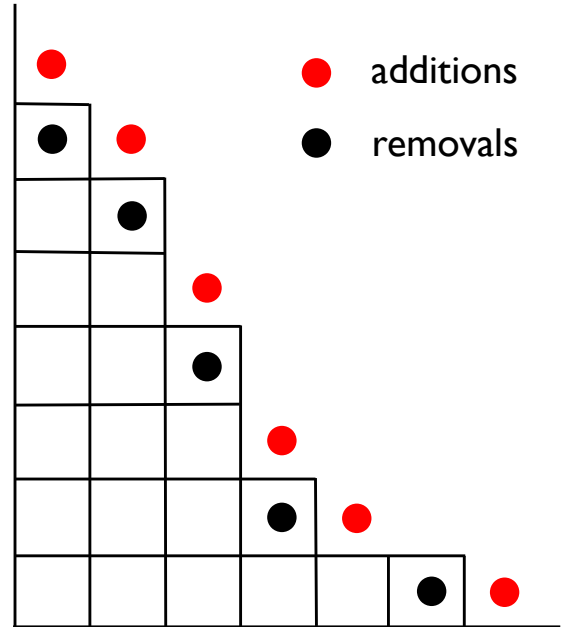


FIG. 4: Diffusive growth of arbitrary partitions—additions and removals of squares occur with the same rate. Shown is the Young diagram of the partition  $21 = 7 + 6 + 4 + 2 + 1 + 1$  together with 6 spots to which a square can be added and 5 spots from which squares can be removed. There is always one more spot for addition than for removal, so the average the area is  $\langle S \rangle = t$  implying that the typical size grows diffusively as  $\sqrt{t}$ .

## VI. DIFFUSIVE GROWTH

In the previous sections we considered growing partitions (only deposition events were allowed). We investigated partitions of different types: arbitrary partitions, partitions with unequal parts (strict partitions), and generally partitions with height difference  $\geq r$ . The growth was always ballistic, see (36).

One can allow both additions and removals of squares, requiring of course that the evolving Young diagram remains the Young diagram of the prescribed type. If the addition rate exceeds the evaporation rate, the growth remains ballistic. A qualitatively different diffusive growth occurs if additions and removals of squares proceed with equal rates. Figure 4 illustrates this process in the case of arbitrary partitions. The number of positions where new squares can be added always exceeds by one the number of positions from which squares can be removed. Hence the average area increases linearly in time:

$$\langle S \rangle = t \quad (43)$$

In the case of arbitrary partitions the above evolution process maps onto the symmetric simple exclusion process (SSEP) for which the diffusion equation,  $n_t = n_{zz}$ ,

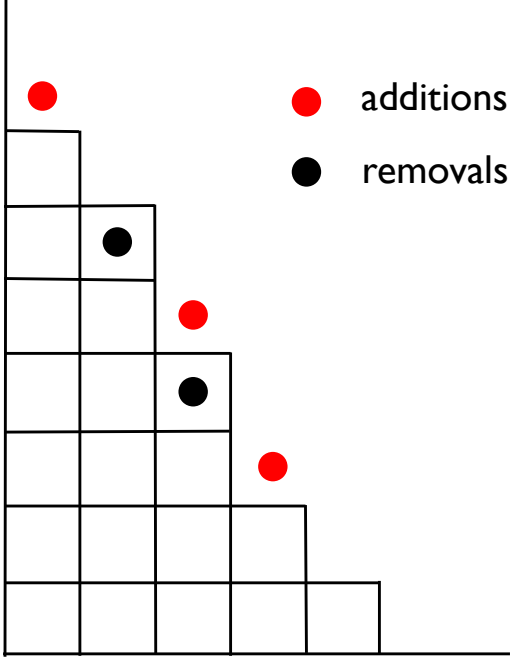


FIG. 5: Diffusive growth of strict partitions. Shown is the Young diagram of the partition  $20 = 7 + 6 + 4 + 2 + 1$  with unequal parts together with 3 possible spots for additions and 2 squares which can be removed. In this example  $m_5 = 1$  and  $m_6 = 0$ , so the right-most square cannot be removed since  $m_5 - m_6 \geq 1$  is required.

provides the hydrodynamic description. Solving this equation subject to the initial condition (14) one gets

$$n(z, t) = \frac{1}{2} \text{Erfc}(\zeta), \quad \zeta = \frac{z}{\sqrt{4t}} \quad (44)$$

which in conjunction with (16) give the limit shape.

A diffusive growth of strict partitions (Fig. 5) maps onto the facilitated symmetric simple exclusion process (FSSEP) in which the hopping is facilitated (caused by the nearest neighbor) and symmetric. The hydrodynamic description of the FSSEP is provided by a non-linear diffusion equation

$$\frac{\partial n}{\partial t} = \frac{\partial}{\partial z} \left( \frac{1}{n^2} \frac{\partial n}{\partial z} \right) \quad (45)$$

This description is applicable when  $\frac{1}{2} \leq n \leq 1$ ; for  $n < \frac{1}{2}$ , the FSSEP quickly reaches a jammed state like

$$\dots \bullet \circ \circ \circ \bullet \circ \circ \bullet \circ \circ \circ \bullet \circ \circ \circ \bullet \circ \circ \circ \bullet \circ \circ \dots$$

Thus the FSSEP is characterized by the density-dependent diffusion coefficient  $D(n) = n^{-2}$ . This result can be extracted from the diffusion coefficient characterizing an apparently very different model, a repulsion process [51] which actually has a well-defined hydrodynamic behavior in the entire range  $0 \leq n \leq 1$ . In the density

range  $\frac{1}{2} \leq n \leq 1$  both the repulsion process and the FSSEP have identical structure of the equilibrium states and this allows us to borrow the known result from the analysis [51] of the repulsion process.

Equation (45) and the initial condition (14) admit a self-similar solution

$$n(z, t) = N(\zeta), \quad \zeta = \frac{z}{\sqrt{4t}} \quad (46)$$

The governing partial differential equation (45) reduces to an ordinary differential equation

$$(N^{-2}N')' + 2\zeta N' = 0 \quad (47)$$

where prime denotes differentiation with respect to  $\zeta$ . We must solve (47) in the region  $-\infty < \zeta < v$ . The boundary condition at  $\zeta \rightarrow -\infty$  is

$$N(-\infty) = 1 \quad (48)$$

The density at the right boundary is

$$N(v) = \frac{1}{2} \quad (49)$$

We need an additional boundary condition since  $v$ , the (scaled) position of the right boundary is unknown. The current through it is given by  $-D(n)n_z = -N^{-2}N'/\sqrt{4t}$  and it should be equal to  $N \frac{d}{dt} v \sqrt{4t} = Nv/\sqrt{t}$ . Therefore  $N' = -2N^3v$ , or

$$N'(v) = -\frac{v}{4} \quad (50)$$

Numerically solving (47) subject to the boundary conditions (48)–(50) one finds  $v \approx 0.564189$ . Therefore

$$X_{\max} = 2v\sqrt{t} \approx 1.12838\sqrt{t} \quad (51)$$

There is one more spot for addition than for removal of squares, so the average area is again given by (43). This growth law also follows from the diffusion equation (45) thereby providing a consistency check. Indeed, the average area varies with unit rate:

$$\frac{d\langle S \rangle}{dt} = - \int_{-\infty}^{v\sqrt{4t}} dz n^{-2} n_z = - \int_1^{\frac{1}{2}} \frac{dN}{N^2} = 1 \quad (52)$$

Generally for the diffusive growth of partitions satisfying the requirement  $m_j - m_{j+1} \geq r$  the governing diffusion equation reads

$$\frac{\partial n}{\partial t} = \frac{\partial}{\partial z} \left[ \frac{1}{(rn - r + 1)^2} \frac{\partial n}{\partial z} \right] \quad (53)$$

This hydrodynamic description is applicable in the density range  $\frac{r}{r+1} \leq n \leq 1$  and the diffusion coefficient is again established through the relation to the generalized repulsion process [37, 51]. The solution has again a self-similar form (46). Therefore the scaling function satisfies

$$[(rN - r + 1)^{-2}N']' + 2\zeta N' = 0 \quad (54)$$

The boundary conditions on the right edge are

$$N(v) = \frac{r}{r+1}, \quad N'(v) = -v \frac{2r}{(r+1)^3} \quad (55)$$

Numerically solving (54) subject to (48) and (55) one can find  $v = v(r)$ .

Finally, let us discuss fluctuations. In the case of arbitrary partitions the mapping onto the SSEP is a significant simplification since fluctuations in lattice gases with constant diffusion coefficients are more amenable to analytical treatment (see [63, 64] for a review of fluctuations in diffusive lattice gases). Fluctuations in the FSSEP, and generally in lattice gases with density-dependent diffusion coefficients, are very challenging.

For arbitrary diffusively growing partitions one can probe fluctuations of the area [38]. These fluctuations turn out to be strongly non-Gaussian. The cumulants grow as  $\langle S^p \rangle_c = A_p t^{(p+1)/2}$  in the  $t \rightarrow \infty$  limit. For  $p \leq 4$ , the amplitudes  $A_p$  have been determined analytically [38]. For diffusively growing strict partitions one can try to generalize the perturbative approach [65] to the determination of the variance and extend the computations of Ref. [38] to strict partitions. This is perhaps doable, although the lack of explicit analytical solution to (47) possesses an extra challenge.

Fluctuations of the width and height might be more tractable. In the case of arbitrary partitions, the average displacement of the right-most particle can be estimated from the criterion

$$\int_{\langle w_t \rangle}^{\infty} dz n(z, t) \sim 1 \quad (56)$$

Combining (44) and (56) one gets

$$\langle w_t \rangle \simeq \sqrt{2t \ln t} \quad (57)$$

One can heuristically estimate the variance of the width,  $\langle w_t^2 \rangle - \langle w_t \rangle^2$ , by arguing that it scales as the square of the average gap  $\langle g_t \rangle$  between the right-most particle and the following particle. This gap can be estimated from the criterion  $\int_{\langle w_t \rangle - \langle g_t \rangle}^{\langle w_t \rangle} dz n(z, t) \sim 1$  to give

$$\langle w_t^2 \rangle - \langle w_t \rangle^2 \sim \frac{t}{\ln t} \quad (58)$$

More precise results are available in the situation when particles undergo Brownian motions [66], while the relevant case of the SSEP is studied in [67].

In the case of strict diffusively growing Young diagrams we use again the mapping illustrated in (41), now it is the mapping of the FSSEP onto the half-SSEP. A similar model has been studied in the past—the SSEP with a localized source, more precisely the infinitely strong source into the origin [68–71]. The average number of particles in the half-SSEP, which is identical to the average width of strict diffusively growing Young diagrams, is easy to compute:  $\langle w_t \rangle \simeq 2\sqrt{t/\pi}$ . The variance (computed in [68, 69] using more advanced techniques) is

$$\langle w_t^2 \rangle - \langle w_t \rangle^2 \simeq 2(3 - \sqrt{8})\sqrt{t/\pi} \quad (59)$$

Therefore fluctuations scale as  $t^{1/4}$  and

$$w_t = 2\sqrt{t/\pi} + t^{1/4}\mathcal{W} \quad (60)$$

The challenge is to determine the (non-Gaussian) random distribution  $\mathcal{W}$ .

## VII. CONCLUDING REMARKS

We computed limit shapes for an infinite family of growing two-dimensional Young diagrams parametrized by a non-negative integer  $r$ , the minimal difference between the heights of adjacent columns. In the situation when additions and removals of squares proceed with equal rates, the growth is diffusive; we determined the corresponding limit shapes, although not explicitly as they are expressed through analytically insoluble ordinary differential equations.

Generally, limit shapes characterizing growing objects are often computable. For instance, infinitely many limit shapes were computed [37] for the melting Ising crystals on the square lattice with ferromagnetic spin-spin interactions; these limit shapes are parametrized by the range of interaction. The major challenge is the extension to the three-dimensional growing Young diagrams. The mapping of the growing interface in three dimensions onto a two-dimensional lattice gas is possible, but it has not yet led to a scheme allowing to extract a limit shape.

I am grateful to K. Mallick for useful discussions. I also benefitted from the correspondence with G. Barraquand, I. Corwin, K. Mallick and T. Sasamoto. This work was supported by the BSF Grant No. 2012145.

- 
- [1] L. Euler, *Introduction to Analysis of the Infinite* (Springer, New York, 1988).
  - [2] G. H. Hardy and S. Ramanujan, Proc. London Math. Soc. **17**, 75 (1918).
  - [3] H. Rademacher, Proc. London Math. Soc. **43**, 241 (1937).
  - [4] T. M. Apostol, *Modular Functions and Dirichlet Series*

*in Number Theory*, 2nd ed. (Springer-Verlag, New York, 1990).

- [5] G. E. Andrews, *The Theory of Partitions* (Cambridge University Press, New York, 1976).
- [6] W. Fulton, *Young Tableaux, with Applications to Representation Theory and Geometry* (Cambridge University



- Press, New York, 1997).
- [7] I. G. Macdonald, *Symmetric Functions and Hall Polynomials* (Oxford University Press, Oxford, 1999).
  - [8] D. Romik, *The Surprising Mathematics of Longest Increasing Subsequences* (Cambridge University Press, New York, 2015).
  - [9] H. A. Bethe, Phys. Rev. **50**, 332 (1936).
  - [10] H. N. V. Temperley, Proc. R. Soc. A **199**, 361 (1949).
  - [11] F. Y. Wu, G. Rollet, H. Y. Huang, J. M. Maillard, C. K. Hu, and C. N. Chen, Phys. Rev. Lett. **76**, 173 (1996).
  - [12] M. N. Tran, M. V. N. Murthy, and R. K. Bhaduri, Ann. Phys. **311**, 204 (2004).
  - [13] A. Kubasiak, J. K. Korbicz, J. Zakrzewski, and M. Lewenstein, EPL **72**, 506 (2005).
  - [14] A. Comtet, S. N. Majumdar, and S. Ouvry, J. Phys. A **40**, 11255 (2007).
  - [15] N. Destainville and S. Govindarajan, J. Stat. Phys. **158**, 950 (2015).
  - [16] A. Okounkov, Bull. Amer. Math. Soc. **53**, 187 (2016).
  - [17] P. A. MacMahon, *Combinatory analysis*, Vol. I & II (Cambridge University Press, Cambridge, 1915–16).
  - [18] H. N. V. Temperley, Proc. Cambridge Philos. Soc. **48**, 683 (1952).
  - [19] A. M. Vershik and S. V. Kerov, Funct. Anal. Appl. **19**, 21 (1985).
  - [20] J.-P. Marchand and Ph. A. Martin, J. Stat. Phys. **44**, 491 (1986).
  - [21] A. M. Vershik, Funct. Anal. Appl. **30**, 90 (1996); A. M. Vershik, J. Math. Sci. **119**, 165 (2004).
  - [22] A. M. Vershik and Yu. V. Yakubovich, Moscow Math. J. **1**, 457 (2001).
  - [23] S. Shlosman, J. Math. Phys. **41**, 1364 (2000).
  - [24] P. L. Krapivsky, S. Redner, and J. Tailleur, Phys. Rev. E **69**, 026125 (2004).
  - [25] A. M. Vershik and S. V. Kerov, Soviet Math. Dokl. **18**, 527 (1977).
  - [26] R. Cerf and R. Kenyon, Commun. Math. Phys. **222**, 147 (2001).
  - [27] A. Okounkov and N. Reshetikhin, J. Amer. Math. Soc. **16**, 581 (2003).
  - [28] H. Cohn, M. Larsen, and J. Propp, New York J. Math. **4**, 137 (1998).
  - [29] H. Cohn, R. Kenyon, and J. Propp, J. Amer. Math. Soc. **14**, 297 (2001).
  - [30] A. Okounkov and N. Reshetikhin, Commun. Math. Phys. **269**, 571 (2007).
  - [31] R. Kenyon and A. Okounkov, Acta Math. **199**, 263 (2007).
  - [32] P. Di Francesco and N. Reshetikhin, Commun. Math. Phys. **309**, 87 (2012).
  - [33] H. Rost, Theor. Prob. Rel. Fields **58**, 41 (1981).
  - [34] T. M. Liggett, *Interacting Particle Systems* (Springer, New York, 1985).
  - [35] D. Kandel and E. Domany, J. Stat. Phys. **58**, 685 (1990).
  - [36] M. Barma, J. Phys. A **25**, L693 (1992).
  - [37] P. L. Krapivsky and J. Olejarz, Phys. Rev. E **87**, 062111 (2013).
  - [38] P. L. Krapivsky, K. Mallick, and T. Sadhu, J. Phys. A **48**, 015005 (2015).
  - [39] P. L. Krapivsky, S. Redner and E. Ben-Naim, *A Kinetic View of Statistical Physics* (Cambridge: Cambridge University Press, 2010).
  - [40] P. L. Krapivsky, Phys. Rev. E **85**, 011152 (2012).
  - [41] R. A. Blythe and M. R. Evans, J. Phys. A **40**, R333 (2007).
  - [42] T. Sasamoto and M. Wadati, J. Phys. A **31**, 6057 (1998).
  - [43] K. Klauk and A. Schadschneider, Physica A **271**, 102 (1999).
  - [44] T. Antal and G. M. Schütz, Phys. Rev. E **62**, 84 (2000).
  - [45] G. Lakatos and T. Chou, J. Phys. A **36**, 2027 (2003).
  - [46] L. B. Shaw, R. K. P. Zia, and K. H. Lee, Phys. Rev. E **68**, 021910 (2003).
  - [47] U. Basu and P. K. Mohanty, Phys. Rev. E **79**, 041143 (2009).
  - [48] A. Gabel, P. L. Krapivsky, and S. Redner, Phys. Rev. Lett. **105**, 210603 (2010).
  - [49] A. Comtet, S. N. Majumdar, S. Ouvry, and S. Sabhapandit, J. Stat. Mech. (2007) P10001.
  - [50] A. Comtet, S. N. Majumdar, and S. Sabhapandit, J. Math. Phys. Anal. Geom. **4**, 24 (2008).
  - [51] P. L. Krapivsky, J. Stat. Mech. P06012 (2013).
  - [52] T. Halpin-Healy and Y.-C. Zhang, Phys. Rep. **254**, 215 (1995).
  - [53] M. Prähofer and H. Spohn, “Current fluctuations for the totally asymmetric exclusion process,” pp. 185–204 in: *In and Out of Equilibrium: Probability with a Physics Flavor*, ed. by V. Sidoravicius (Birkhäuser, Boston, 2006).
  - [54] I. Corwin, Random Matrices Theory Appl. **1**, 1130001 (2012).
  - [55] T. Halpin-Healy and K. A. Takeuchi, J. Stat. Phys. **160**, 794 (2015).
  - [56] K. Johansson, Commun. Math. Phys. **209**, 437 (2000).
  - [57] K. Mallick, unpublished.
  - [58] J. Baik, G. Barraquand, I. Corwin, and T. Suidan, “Facilitated exclusion process and pfaffian Schur processes,” preprint.
  - [59] J. Baik and E. M. Rains, Duke Math. J. **109**, 1 (2001) and Duke Math. J. **109**, 205 (2001).
  - [60] J. Baik and E. M. Rains, “Symmetrized random permutations,” pp. 1–19 in: *Random matrix models and their applications* (Cambridge: Cambridge University Press, 2001).
  - [61] T. Sasamoto and T. Imamura, J. Stat. Phys. **115**, 749 (2004); T. Sasamoto, J. Stat. Mech. P07007 (2007).
  - [62] G. Barraquand and I. Corwin, arXiv:1501.03445.
  - [63] B. Derrida, J. Stat. Mech. P07023 (2007).
  - [64] L. Bertini, A. De Sole, D. Gabrielli, G. Jona-Lasinio, and C. Landim, Rev. Mod. Phys. **87**, 593 (2015).
  - [65] P. L. Krapivsky and B. Meerson, Phys. Rev. E **86**, 031106 (2012).
  - [66] S. Sabhapandit, J. Stat. Mech. L05002 (2007).
  - [67] K. Mallick and T. Sasamoto, in preparation.
  - [68] J. E. Santos and G. M. Schütz, Phys. Rev. E **64**, 036107 (2001).
  - [69] P. L. Krapivsky, Phys. Rev. E **86**, 041103 (2012).
  - [70] C. A. Tracy and H. Widom, J. Math. Phys. **54**, 103301 (2013).
  - [71] P. L. Krapivsky and D. Stefanovic, J. Stat. Mech. P09003 (2014).